# AN ALGORITHM FOR REMOTE SENSING OF WATER COLOR FROM SPACE

M. VIOLLIER, D. TANRÉ, P. Y. DESCHAMPS

*Laboratoire d'optique atmosphérique (ERA 466) Université des sciences et techniques de Lille, U.E.R. de Physique Fondamentale 59655 Villeneuve d'Ascq CEDEX – (France)*

(Received 12 October, 1979)

**Abstract.** The ocean color algorithm proposed in this paper takes into account the effects of Rayleigh and aerosol scattering. The inherent reflectance and the diffuse transmittance of the Rayleigh atmosphere are expressed as functions of optical thickness and satellite measurement geometry with the aid of simple and accurate formulas. In the case of a turbid atmosphere, from which the aerosol optical thickness is unknown, the aerosol contribution is estimated with the aid of a measurement in a channel where the ocean is a blackbody (in the red or near infrared). If the relationship between the ocean color and the chlorophyll-like pigment concentration is assumed to be known at sea level, it is shown that the chlorophyll-like pigment concentration at an open ocean site can be determined from space to within a factor of 1.5 to 3 (uncertainty equal to 0.2 to 0.5 log interval), depending on the atmospheric turbidity.

## 1. Introduction

Several airborne experiments have already shown the feasibility of ocean color measurements in the determination of the relative chlorophyll richness of water masses (Clarke *et al.*, 1970; Arvesen *et al.*, 1973; Miller *et al.*, 1977; Wilson *et al.*, 1978; Viollier *et al.*, 1978a). Most of the experiments were carried out at low altitude in order to minimize the masking effects of the atmosphere in the spectral range for which the ocean has a useful spectral signature (0.4 to 0.7 μm).

The realization of these ocean color measurements from space, notably by the CZCS experiment (Coastal Zone Color Scanner, Hovis, 1978) poses the problem of eliminating atmospheric influences in a more crucial and complex way. Examples of the magnitude of this effect are given by the theoretical computations of Kattawar and Humphreys (1976), and by the experimental results of Hovis *et al.* (1973). The main difficulty in the correction of atmospheric effects is due to the presence of aerosol, for which optical characteristics are variable in both time and space. Curran (1972) has evaluated the accuracy required of aerosol optical thickness measurements for chlorophyll content determinations. Gordon (1978) has proposed the correction of the aerosol influence by measurements at 0.7 μm or longer, where the ocean becomes a blackbody. This method assumes (1) the independence of scattering effects due to molecules and aerosols, (2) the linear dependence of the aerosol effect upon optical thickness. These hypotheses are verified in the present article by means of accurate computations of diverse terms of atmospheric perturbation, and simple formulas have been found to facilitate quick and accurate correction. The developed atmospheric correction algorithm is finally applied to the measurement of chlorophyll-like pigment concentration in accordance with the method already proposed

*Boundary-Layer Meteorology* **18** (1980) 247–267. 0006-8314/80/0183-0247$03.15.

by Viollier *et al.* (1978a), and the accuracy with which chlorophyll-like pigment concentration can be determined from satellites is estimated.

## 2. Model

The radiative transfer in the ocean-atmosphere system is modelled in the following way. The radiance $I_\lambda((\theta, \phi), (\theta_0, \phi_0))$ measured from space, at wavelength $\lambda$, is systematically expressed as a reflectance

$$R_\lambda((\theta, \phi), (\theta_0, \phi_0)) = \frac{\pi I_\lambda((\theta, \phi), (\theta_0, \phi_0))}{E_{0\lambda} \cos \theta_0} \tag{1}$$

where $E_{0\lambda}$ is the solar spectral irradiance at the top of the atmosphere, and $(\theta, \phi)$ and $(\theta_0, \phi_0)$ represent the observation and incidence directions. Notation will be simplified by deleting subscript $\lambda$ from optical terms. The several contributions of the measured reflectance can be split up in the following way:

$$R = R_a + R_0 + R_{a0} + R_{0a} + R' \tag{2}$$

where, in accordance with Figure 1, each term represents a possible radiation pathway:

- $R_a$: radiation scattered uniquely by the atmosphere (without an ocean reflection component).
- $R_0$: direct radiation reflected by the ocean (without atmospheric scattering).
- $R_{a0}$: diffuse sky radiation reflected towards the satellite.
- $R_{0a}$: direct radiation reflected and then scattered towards the satellite.
- $R'$: reflected radiation which has been reflected and/or scattered more than twice.

The last term, $R'$, is negligible when the target surface reflectance is a few percent, which is generally the case in measurement of ocean color. Terms $R_0$, $R_{a0}$ and $R_{0a}$ are all proportional to the ground reflectance $\rho$ for an uniform Lambertian ground reflectance, and it is then possible to write

$$R = R_a + \rho T \tag{3}$$

and in this way to define the diffuse transmittance $T$.

### Ocean reflectance

The ocean reflectance $\rho_0$ can be considered to be the addition of a perfectly diffuse reflectance $\rho$ resulting from backscattering from the water mass and a surface specular reflectance $\rho'$ which obeys Fresnel's laws

$$\rho_0((\theta, \phi), (\theta', \phi')) = \rho + \rho'(\theta)\delta(\theta - \theta')\delta(\phi - \phi') \tag{4}$$

where $\delta$ is the Dirac function. This model is valid only for a perfectly calm water surface. When the water surface is rough, the radiation reflected from the surface is no longer sent uniquely in the direction of the specular reflection, but rather is distributed around this direction (see Annex II). Part of this reflected radiation then

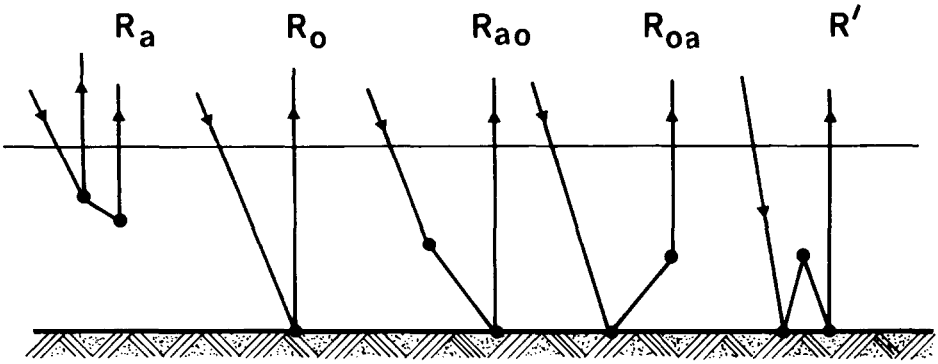


Fig. 1. The different pathways followed by radiation which upwells towards the satellite.

is directly measured by the satellite, and this constitutes the 'glitter' phenomenon. In this study we will suppose that the glitter can be ignored, which assumes the target surface to be perfectly smooth. Furthermore, as most of the surface reflected radiation will thus be sent in the direction of the specular reflection, it will be possible to get good approximate values for $R_{a0}$, $R_{0a}$, and $R'$ by using expression (4).

### Atmospheric absorption and scattering

In the range used for the measure of ocean color, 0.4 to 0.7 μm, the only notably absorbing atmospheric gas is ozone. The absorption due to ozone can be localized in the atmosphere above the scattering layers and its influence can be calculated separately (see Annex I).

In what follows, Rayleigh scattering due to molecules and Mie scattering due to aerosols have been taken into account. Two cases have been studied. The first case was that of a purely Rayleigh atmosphere, and simple and precise formulas for the evaluation of perturbation due to this kind of atmosphere have been developed; in the second case, aerosols (standard aerosol model, from McClatchey 1971) were added to the Rayleigh atmosphere and an attempt was made to demonstrate the linear relationship between optical thickness and the supplementary perturbation introduced by the aerosols.

Computations were made at wavelengths of 450, 550 and 650 nm, which cover the useful interval in the measure of ocean color (the CZCS channels are at 443, 520, 550, 670 and 750 nm). In what follows it is to be borne in mind that the spectral reflectance signature of the ocean has an amplitude of a few $10^{-2}$ and that an accuracy on the order of $10^{-3}$ is necessary for the determination of this signature.

## 3. Pure Rayleigh Atmosphere

The resolution of radiative transfer in a Rayleigh atmosphere poses no particular problem. Certain of these results can be found in the form of tables (Sekera and Kahle, 1966). Nevertheless, neither exact computer calculation nor the reading of a

table is entirely satisfactory for the pixel-by-pixel correction of the satellite image. What is really needed is the simplest possible formula giving reflectance with an accuracy of $10^{-3}$.

With this in mind, we have compared the results of exact computations for a plane-parallel atmosphere which were obtained by the successive orders of scattering method (taking polarization into acount), with results obtained with the aid of approximate formulas. This comparison is made for terms $R_a^M$ and $T^M$ of Equation 3 (the superscript $M$ indicating that they refer to a Rayleigh atmosphere).

### Atmospheric reflectance $R_a^M$

This term corresponds to the apparent reflectance which is measured for a perfectly black surface ($\rho = 0$).

Table I gives the results of exact computations for optical thickness corresponding to 450, 550 and 650 nm, incidence angles $\theta_0$ being of 15° and 60°, and observation angle $\theta$ being of 0° and 30° in a plane perpendicular to the plane of incidence ($\phi - \phi_0 = 90°$). These conditions correspond approximately to the geometrical configuration extremes that are possible in the observation of ocean color from space. The results are given for the exact computation, with and without polarization: as has already been pointed out (Plass *et al.*, 1976), it is necessary to account for polarization introduced by Rayleigh scattering in order to obtain the necessary accuracy.

For small optical thickness, multiple scattering becomes negligible and the calculation of single scattering gives a value $R_a^{M(1)}$ close to the exact value $R_a^M$ with

$$R_a^{M(1)} = \frac{p(\chi)}{4(\mu + \mu_0)}\left[1 - \exp - \tau^M\left(\frac{1}{\mu} + \frac{1}{\mu_0}\right)\right] \tag{5}$$

where $\chi = \pi - \arccos(\cos\theta \cos\theta_0 + \sin\theta \sin\theta_0 \cos(\phi - \phi_0))$ is the scattering angle, $\mu_0 = \cos\theta_0$, $\mu = \cos\theta$, or, since $\tau$ is small,

$$R_a^{M(1)} = \frac{p(\chi)}{4\mu\,\mu_0}\tau^M \tag{6}$$

with

$$p(\chi) = \tfrac{3}{4}(1 + \cos^2\chi) \tag{7}$$

for Rayleigh scattering.

The latter approximation was used to obtain the values recorded in Table I (column 3). It is interesting to note that the approximate expression (Equation 6) for single scattering gives much better results than does the exact expression (Equation 5). By using the approximate expression (Equation 6), residual errors of a few 0.001 occur, which can be very simply tabulated with an accuracy of 0.001 since the majority of the geometry-associated variations were taken into account in the term $p(\chi)/\mu\mu_0$. Other equations can be found which more exactly account for multiple scattering, but the accuracy obtained is hardly better than the accuracy obtained by

TABLE I

Comparisons between alternative computations of atmospheric reflectances due to Rayleigh scattering ($R_a^M$) both without and with specular reflectance from the sea surface, without and with polarization, and comparison between exact and approximate computations: 1 – exact without polarization; 2 – exact with polarization; 3 – approximated by Equation 6; 4 – exact with polarization; and 5 – approximated by Equation 9

| | | $\lambda$ | Without specular reflection | | | With specular reflection | |
|---|---|---|---|---|---|---|---|
| | | (nm) | 1 | 2 | 3 | 4 | 5 |
| $\theta = 0$ | $\theta_0 = 15$ | 450 | 0.0791 | 0.0838 | 0.0809 | 0.0884 | 0.0842 |
| | | 550 | 0.0355 | 0.0367 | 0.0356 | 0.0391 | 0.0370 |
| | | 650 | 0.0181 | 0.0184 | 0.0180 | 0.0193 | 0.0187 |
| | $\theta_0 = 60$ | 450 | 0.1009 | 0.0988 | 0.1011 | 0.1096 | 0.1091 |
| | | 550 | 0.0453 | 0.0448 | 0.0444 | 0.0506 | 0.0479 |
| | | 650 | 0.0229 | 0.0228 | 0.0225 | 0.0257 | 0.0243 |
| $\theta = 30$ | $\theta_0 = 15$ | 450 | 0.0816 | 0.0846 | 0.0822 | 0.0903 | 0.0855 |
| | | 550 | 0.0364 | 0.0373 | 0.0361 | 0.0397 | 0.0375 |
| | | 650 | 0.0185 | 0.0187 | 0.0183 | 0.0199 | 0.0190 |
| | $\theta_0 = 60$ | 450 | 0.1119 | 0.1098 | 0.1109 | 0.1209 | 0.1197 |
| | | 550 | 0.0501 | 0.0496 | 0.0487 | 0.0555 | 0.0526 |
| | | 650 | 0.0253 | 0.0252 | 0.0247 | 0.0279 | 0.0267 |

equation 6 in the previously defined observation range. Equation 6 is simple, and seems to give the best results.

## SPECULAR REFLECTION

The ocean reflection model was described in Section 2. The greater part of the radiation is reflected in the direction of specular reflection. Part of this radiation interacts with the atmosphere by scattering and makes a significant contribution to measured radiation.

This contribution can be approximated with sufficient accuracy by the following formula:

$$R_{\text{spec}} = (\rho'(\theta) + \rho'(\theta_0)) \frac{p(\chi')}{4\mu\,\mu_0} \tau^M \tag{8}$$

(with $p(\chi') = p(\chi)$ for $\chi' = \pi - \chi$) which accounts for radiation reflected after scattering and radiation scattered after reflection, with reflection coefficients $\rho'(\theta)$ and $\rho'(\theta_0)$. For nearly vertical sightings, $\rho'(\theta)$ is equal to 0.02, and the term $R_{\text{spec}}$ is then of the order of 0.004 at 450 nm.

This term can easily be incorporated into $R_a$ (in place of Equation 6) which becomes

$$R_a^{M(1)} = (1 + \rho'(\theta) + \rho'(\theta_0)) \frac{p(\chi)}{4\mu\,\mu_0} \tau^M . \tag{9}$$

With Table I (columns 4 and 5), it is possible to test the validity of this expression as compared with the exact computation. Differences of a few 0.001 exist, which can easily be tabulated as a function of the geometry of the problem.

DIFFUSE TRANSMITTANCE $T^M$

For a uniform Lambertian ground reflectance, the Rayleigh diffuse transmittance is defined by Equations 2 and 3:

$$\rho T^M = R_0^M + R_{a0}^M + R_{0a}^M \tag{10}$$

and the analytical expressions for the terms $R_0^M$, $R_{a0}^M$, $R_{0a}^M$ are

$$R_0^M = \rho e^{-\tau^M/\mu_0} e^{-\tau^M/\mu} \tag{11}$$

$$R_{a0}^M = \rho E_a^M e^{-\tau^M/\mu} \tag{12}$$

$$R_{0a}^M = \rho (E_a^M + E_S^M) t^M(\mu) \tag{13}$$

where $t^M(\mu)$ is the appropriate transmittance and $E_S^M$ and $E_a^M$ are respectively the direct and diffuse components of the downwelling normalized irradiance. In accordance with the above conventions, each term is normalized to the incident irradiance outside of the atmosphere, $\mu_0 E_0$, divided by $\pi$; $E_S^M$ and $E_a^M$ are thus dimensionless transmission terms

$$E_S^M = e^{-\tau^M/\mu_0} \tag{14}$$

$$E_a^M = \tfrac{1}{2}(1 - e^{-\tau^M/\mu_0}). \tag{15}$$

Equation 15 is exact for only the single scattering approximation, but this approximation still gives good results when $\tau^M$ is not too large. The expression of the transmittance $t^M(\mu)$ is found to be identical to the expression of $E_a^M$:

$$t^M(\mu) = \tfrac{1}{2}(1 - e^{-\tau^M/\mu}). \tag{16}$$

Combining equations 11 to 16 yields

$$R_0^M + R_{a0}^M + R_{0a}^M = (\rho/4)(1 + e^{-\tau/\mu})(1 + e^{-\tau/\mu_0}) \tag{17}$$

which provides an expression for diffuse transmittance as previously defined by Equation 10

$$T^M(\mu, \mu_0) = \tfrac{1}{4}(1 + e^{-\tau^M/\mu})(1 + e^{-\tau^M/\mu_0}). \tag{18}$$

This formula is used further in the text (Table VI, column 3) and gives excellent accuracy in the retrieval of ground reflectances from synthetic data of $R$.

This model assumes the ground reflectance $\rho$ to be uniform over horizontal distances of at least several kilometers. Ocean reflectance obviously is not completely uniform since fronts, eddies and various patches are present. Ocean reflectance variations are nevertheless small enough for the above model to remain valid as a first approximation. This is not the case for areas very close to the coast

where the change in reflectances between water and land is so large as to invalidate the model. Specific atmospheric corrections which acccount for this particular non-uniform case have not yet been developed.

If this limitation is accepted, formulas 9 and 18 are useful in the elimination of the influence of Rayleigh scattering.

## 4. Turbid Atmosphere

Aerosol scattering causes an additional perturbation of reflectance $R_a$ and diffuse transmittance $T$. In marine or continental zones, the nature of aerosols can be extremely varied: water droplets, industrial or volcanic dust, etc. To study all possible cases present in nature would be impossible. An attempt thus will be made to demonstrate the general laws of radiative transfer in a turbid atmosphere with the aid of a standard aerosol model.

### Aerosol model

Computations for an atmosphere containing aerosols were made using the standard model of McClatchey *et al.* (1971). For this model, particle characteristics are independent of altitude. The particles are assumed to be spherical, non-absorbing, of optical index $m = 1.50$, of the following size distribution:

$$n(r) = 0 \quad \text{if} \quad r < 0.02\ \mu\text{m}$$

$$n(r) = 10^{-4}C \quad \text{if} \quad 0.02 < r < 0.1\ \mu\text{m}$$

$$n(r) = Cr^{-4} \quad \text{if} \quad 0.1 < r < 10\ \mu\text{m}$$

$$n(r) = 0 \quad \text{if} \quad r > 10\ \mu\text{m}$$

$$C = 8.83\ 10^{-5}\ \mu\text{m}^{-4}.$$

The value of the phase function deduced from this model are presented in Table II.

McClatchey *et al.* (1971) selected two atmospheric aerosol distributions, one representative of a clear sky and one of a hazy sky. The two models correspond to horizontal visibilities of respectively 23 and 5 km. The optical thicknesses of the aerosols in these two models are presented in Table III.

### Linearity of $R_a^A$ as compared with $\tau^A$

Tanré and Herman (1978) have demonstrated that for nearly vertical sightings ($\theta < 15°$) and aerosol optical thicknesses smaller than 0.5, the reflectance for a turbid atmosphere can be written as

$$R_a = R_a^M + R_a^A \tag{19}$$

where $R_a^A$ is the reflectance due to a hypothetical atmosphere containing only aerosols; the term including the Rayleigh-aerosol interaction was found to be less than 3%.

TABLE II

Phase function of the aerosol model of McClatchey *et al.* (1971). The ratio between $p^A(\chi)$ at 450 and 650 nm (last column) emphasizes the dependence of $p^A(\chi)$ upon wavelength, particularly in backward directions. The angles chosen, $\chi$, are those used in the approximate computations presented in this paper

| Phase angle $\chi$ | Phase function $p^A(\chi)$ 450 nm | 550 nm | 650 nm | Ratio $p^A_{450}(\chi)/p^A_{650}(\chi)$ |
|---|---|---|---|---|
| 15° | 8.54 | 8.39 | 8.31 | 1.03 |
| 41° | 1.93 | 1.93 | 1.92 | 1.00 |
| 60° | 0.80 | 0.81 | 0.82 | 0.97 |
| 120° | 0.141 | 0.152 | 0.160 | 0.87 |
| 139° | 0.153 | 0.166 | 0.175 | 0.88 |
| 165° | 0.328 | 0.337 | 0.345 | 0.95 |

Unlike the Rayleigh reflectance, it would be superfluous to look for approximations of $R_a^A$ as a function of aerosol optical thickness and phase function. That would not resolve the problem because the aerosol optical parameters are exceedingly variable in time and space. An attempt should instead be made to correlate the atmospheric correction directly with a satellite measurement. Gordon (1978) suggests a linear dependence of $R_a$ on $\tau^A$. Thus if one knows the spectral dependence of $\tau^A$, the value of $R_{a\lambda}^A$ at a given wavelength can be deduced from $R$ measured at a different wavelength, i.e., in the red where the radiance backscattered by the ocean becomes nil.

This is illustrated in Table IV which presents the results of exact computations of $R_a^A$ for a vertical sighting ($\theta = 0$), and for three solar angles ($\theta_0 = 15°$, 41.41° and 60°), as well as by Table V, which presents the differences between the exact and approximate computations of $R_a^A$ at 450 nm. The computations were made for the two cases, clear and hazy. The approximate determination of $R_a^A$ at 450 nm ($R_{a450}^A$) is deduced from the exact value of $R_{a650}^A$ by use of the linear relationship between $R_a^A$ and $\tau^A$.

Two equations were tried, first

$$R_{a450}^A = \varepsilon R_{a650}^A \tag{20}$$

TABLE III

Rayleigh optical thickness from Hoyt (1977), and aerosol optical thickness for the clear and hazy models from McClatchey *et al.* (1971)

| $\lambda$ (nm) | 450 | 550 | 650 |
|---|---|---|---|
| $\tau^M$ | 0.2157 | 0.0948 | 0.0481 |
| $\tau^A$ Clear | 0.2801 | 0.2348 | 0.2011 |
| $\tau^A$ Hazy | 0.9305 | 0.7801 | 0.6681 |

TABLE IV

Turbid atmosphere: exact computations of the aerosol reflectance $R_a^A$. The zenith solar angles $\theta_0$ are 15, 41.4 and 60°. The sighting is vertical ($\theta = 0$). $R_a^A$ includes the Rayleigh-aerosol interaction

| | | | |
|---|---|---|---|
| *Clear Atmosphere* | | | |
| λ (nm) | $\theta_0 = 15°$ | $\theta_0 = 41.41°$ | $\theta_0 = 60°$ |
| 450 | 0.0212 | 0.0200 | 0.0293 |
| 550 | 0.0200 | 0.0176 | 0.0260 |
| 650 | 0.0182 | 0.0154 | 0.0226 |
| *Hazy Atmosphere* | | | |
| 450 | 0.0765 | 0.0802 | 0.1039 |
| 550 | 0.0704 | 0.0713 | 0.0972 |
| 650 | 0.0631 | 0.0623 | 0.0868 |

where $\varepsilon$ is the optical thickness ratio

$$\varepsilon = \tau^A(450)/\tau^A(650); \tag{21}$$

and second

$$R^A_{a450} = \varepsilon' R^A_{a650} \tag{22}$$

where $\varepsilon' = 0.9\varepsilon$.

In this case the factor 0.9 takes into account the average ratio of the phase function at 450 and 650 nm at the angles of backscattered radiation (see column 5 of Table II). In Table V it is seen that the use of coefficient $\varepsilon' = 0.9\varepsilon$ instead of $\varepsilon$ notably reduces the differences, and this is of particular interest in the 'hazy' model. For the 'clear'

TABLE V

Disparity (in absolute value) between the exact value of $R_a^A$ at 450 nm and the value as approximated by

$R^A_{a450} = \varepsilon R^A_{a650}$ where $\varepsilon = \dfrac{\tau^A_{450}}{\tau^A_{650}}$ column (1)

$R^A_{a450} = \varepsilon' R^A_{a650}$ where $\varepsilon' = 0.9\varepsilon$ column (2)

| | $\theta_0$ | (1) | (2) |
|---|---|---|---|
| *Clear* | 15° | +0.0041 | +0.0015 |
| | 41.4° | +0.0014 | −0.0007 |
| | 60° | +0.0022 | −0.0011 |
| *Hazy* | 15° | +0.0114 | +0.0023 |
| | 41.4° | +0.0066 | −0.0024 |
| | 60° | +0.0170 | +0.0046 |

model, the differences between exact and approximate computations of $R_a^A$ are about $10^{-3}$, which is equal to the magnitude of the desired accuracy.

The interaction between the specular reflection and the scattering can be incorporated into the expression of $R_a^A$ in the same way as in the study of Rayleigh scattering (Equation 8). $R_a^A$ is roughly given by the single scattering approximation

$$R_a^A = \{p^A(\chi) + (\rho'(\theta) + \rho'(\theta_0))p^A(\chi')\}\frac{\tau^A}{4\mu\,\mu_0} \tag{23}$$

where $\chi'$ and $\chi = \pi - \chi'$ respectively designate the forward and backward scattering directions. Given this equation, it is logical to consider that the previously demonstrated results remain valid, indicating that $R_a^A$ is a linear function of $\tau^A$. The algorithm based on Equation 20 thus remains applicable if the influence of the specular reflection upon the scattered radiation is taken into account.

### Diffuse transmittance $T$

The diffuse transmittance expression (Equation 18) established for Rayleigh scattering is no longer valid in the case of aerosols. Unlike Rayleigh scattering, aerosol scattering is very dissymmetric. Typically 70% of the radiation is scattered forwards in an angle of $\pm 10°$ and can be considered directly transmitted. For an atmosphere containing only aerosols, one can write the approximation

$$R^A = R_a^A + \rho \exp - b\tau^A\left(\frac{1}{\mu_0} + \frac{1}{\mu}\right) \tag{24}$$

where $b$ is a coefficient representing the part of the radiation scattered backward by the aerosols. With the McClatchey aerosol model, the best results were obtained by assuming $b$ to be equal to 0.13.

If we consider the aerosol-Rayleigh mixture, the diffuse transmittance Equation 18 combined with equations 11 to 16 and 24 becomes:

$$T = \tfrac{1}{4}(1 + \exp - \tau^M/\mu_0)(1 + \exp - \tau^M/\mu) - \left[1 - \exp - b\tau^A\left(\frac{1}{\mu} + \frac{1}{\mu_0}\right)\right]\exp - \tau^M\left(\frac{1}{\mu} + \frac{1}{\mu_0}\right). \tag{25}$$

This expression has been used for the retrieval of ground reflectances $\rho$ from synthetic data of $R$. Results of such computations are presented in Table VI for two cases of atmospheric turbidity. The retrieval of $\rho$ is obtained by using Equation 3 in which $R_a$ is assumed to be known. It can be seen that the errors in $\rho$ are less than 0.002 when $\rho$ is smaller than 0.05, which is the case in ocean sightings. The influence of aerosols upon the diffuse atmospheric transmittance thus can easily be calculated with the aid of Equation 25.

TABLE VI

Comparison of initial ($\rho$) and retrieval ($\rho_r$) values of the ocean reflectance supposing that $R_a$ is known and using the expression of the diffuse transmittance (Equation 25). $R$ is the reflectance at the top of the atmosphere. The computations were made for the case in which reflectance $\rho$ is lambertian. The sighting is vertical ($\theta = 0$)

| | | Rayleigh | | Clear | | Hazy | |
|---|---|---|---|---|---|---|---|
| | $\rho$ | $R$ | $\rho_r$ | $R$ | $\rho_r$ | $R$ | $\rho_r$ |
| $\theta_0 = 15°$ | 0 | 0.0838 | — | 0.1050 | — | 0.1603 | — |
| | 0.05 | 0.1247 | 0.0503 | 0.1437 | 0.0507 | 0.1936 | 0.0514 |
| | 0.10 | 0.1662 | 0.1014 | 0.1833 | 0.1026 | 0.2279 | 0.1043 |
| $\theta_0 = 41.41°$ | 0 | 0.0860 | — | 0.1060 | — | 0.1662 | — |
| | 0.05 | 0.1257 | 0.0502 | 0.1430 | 0.0502 | 0.1969 | 0.0500 |
| | 0.10 | 0.1661 | 0.1014 | 0.1808 | 0.1015 | 0.2286 | 0.1017 |
| $\theta_0 = 60°$ | 0 | 0.0988 | — | 0.1281 | — | 0.2027 | — |
| | 0.05 | 0.1362 | 0.0502 | 0.1615 | 0.0487 | 0.2289 | 0.0478 |
| | 0.10 | 0.1742 | 0.1012 | 0.1957 | 0.0986 | 0.2559 | 0.0971 |

## 5. Correction Algorithm

By examining the results of the preceding computations, the following method can be proposed for the elimination of atmospheric influences.

Measured radiances are expressed as reflectance $R(\theta, \phi; \theta_0\phi_0)$ with the aid of Equation 1, and then corrected for ozone absorption effects by a multiplicative factor which is a function of geometry ($\theta$, $\theta_0$) and of the average seasonal ozone quantity (see Annex I).

In what follows, subscript 1 will designate the wavelength for which the ocean is considered a black body, and 2 will designate the wavelength at which the correction is effected. Ocean reflectance $\rho_2$ can be retrieved from the reflectances $R_2$ and $R_1$ measured at the top of the atmosphere by the equation

$$\rho_2 = \{(R_2 - R_{a2}^M) - \varepsilon(R_1 - R_{a1}^M)\}T_2^{-1} . \tag{26}$$

In this equation Rayleigh reflectances $R_{a1}^M$ and $R_{a2}^M$ can be calculated with accuracy (see Equation 9) because they depend only upon optical thickness values $\tau_\lambda^M$ which are constant in time, and upon geometric variables ($\theta_0$, $\phi_0$) and ($\theta$, $\phi$).

Diffuse transmission $T_2$ can also be calculated with accuracy (Equation 25); uncertainty relative to the term $b\tau^A$ is of little consequence in the evaluation of $T_2$, which depends mainly upon Rayleigh scattering. The only unknown in Expression 26 is the coefficient $\varepsilon = \tau_2^A/\tau_1^A$. When lacking contemporary experimental determination of $\varepsilon$, one can use an average derived from a statistical study of on site measurements (see Annex III). The accuracy of the algorithm is limited essentially by the probable differences between the real and estimated values of $\varepsilon$.

The coefficient $\varepsilon$ can vary a great deal. It generally is accepted that $\tau^A(\lambda)$ can be approximated by a power law

$$\varepsilon = \frac{\tau_2^A}{\tau_1^A} = \left(\frac{\lambda_2}{\lambda_1}\right)^{-\alpha}. \tag{27}$$

The parameter $\alpha$ depends mainly upon the aerosol size distribution and theoretically can vary between $-0.2$ and 2 (see, for example, Box and Lo, 1976). This leads to variations of $\varepsilon$ between 0.9 and 3 for the spectral range considered here. Actual measurements show this variation to be less extensive, especially for ocean sites (see Annex III). With the aid of Equation 27, it is easy to establish that the uncertainty $\Delta\rho_2$ in $\rho_2$ can be expressed as a function of the uncertainty $\Delta\alpha$ in $\alpha$ by

$$\Delta\rho_2 = \frac{1}{T_2}\frac{\lambda_1}{\lambda_2} R_{a1}^A \alpha \Delta\alpha . \tag{28}$$

For conditions such as $\lambda_1 = 700$ nm, $\lambda_2 = 450$ nm, $\alpha = 1$ and $\Delta\alpha = 0.3$, calculations for the 'clear' model give an uncertainty $\Delta\rho_2$ of the order of 0.01, which is much greater than desired.

The accuracy is decidedly improved when the measurement is relative, i.e., it is the difference or ratio of reflectances at two neighboring wavelengths ($\lambda_2$ and $\lambda_3$). This yields

$$\Delta(\rho_2 - \rho_3) = \left(\frac{1}{T_2}\frac{\lambda_1}{\lambda_2} - \frac{1}{T_3}\frac{\lambda_1}{\lambda_3}\right) R_{a1}^A \alpha \Delta\alpha . \tag{29}$$

For the same conditions as above, the uncertainty is of the order of 0.001 for $\lambda_2 = 450$ nm and $\lambda_3 = 520$ nm. Significant evaluations of ocean color thus can be made with the aid of relative measurements between two neighboring wavelengths.

## 6. Example of Application

The efficiency of atmospheric corrections has to be evaluated relative to the accuracy necessary in the remote sensing of ocean color, and more specifically, relative to the retrieval of chlorophyll-like pigment content. The term 'chlorophyll-like pigment content' is used rather than 'chlorophyll content', because several different pigments absorb and modify the ocean spectral reflectance. Experimental results previously obtained are used to derive an interpretation model of ocean reflectances and to check the efficiency of the atmospheric corrections.

### Interpretation Model

The results of previous low-altitude airborne experiments yield a relationship between chlorophyll-like pigment content and ocean spectral reflectances. This is illustrated in Figure 2, where the differences of the reflectances at 466 nm and

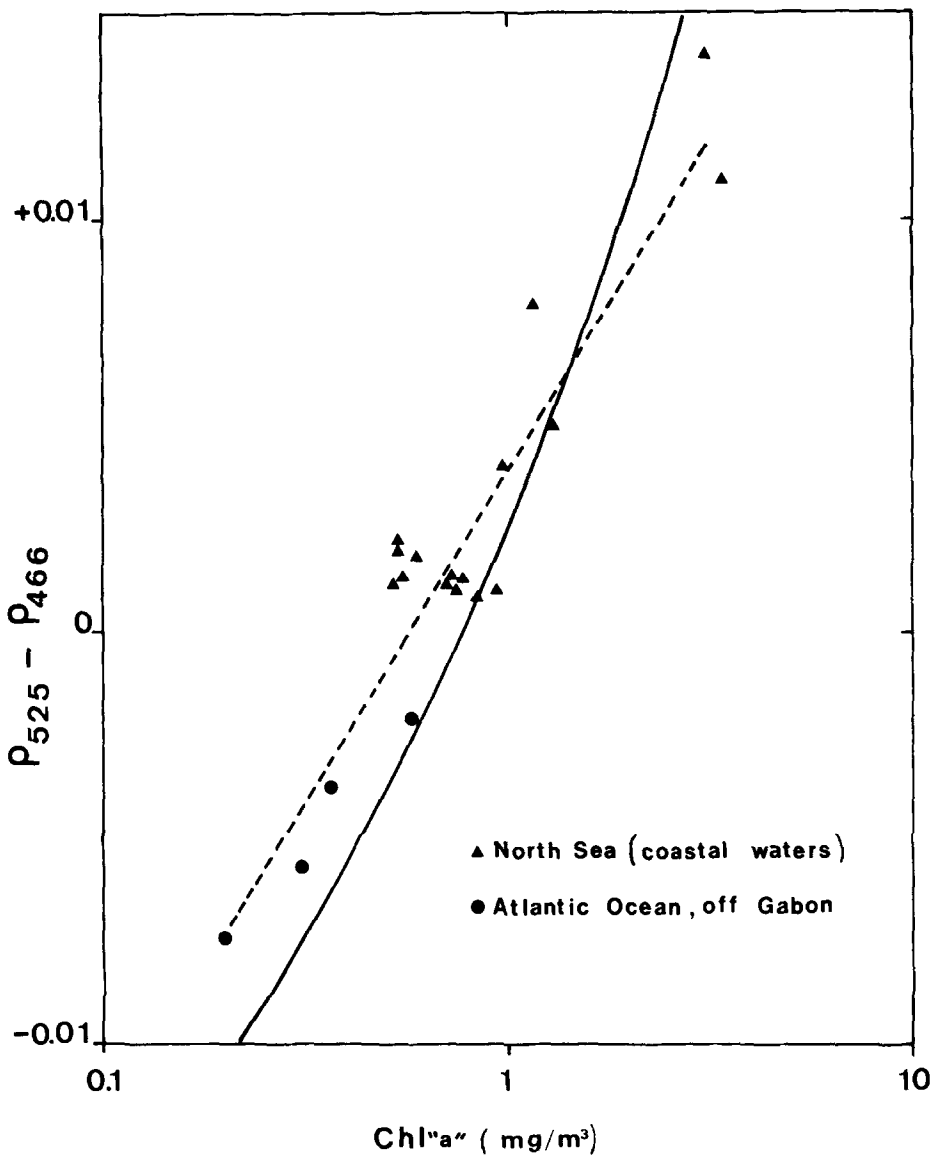


Fig. 2. Difference of reflectances at 525 and 466 nm versus chlorophyll-*a* concentration. *Dashed line*: experimental regression line from airborne measurements of reflectances at low altitude and from *in situ* measurements of chlorophyll-*a*. *Solid line*: theoretical relationship obtained by modelling.

525 nm are plotted versus the chlorophyll-*a* content measured *in situ* by spectrophotometric methods.

Two groups of points are noted. One group of 4 points corresponds to low concentrations of chlorophyll-*a* (from 0.2 to 0.8 mg $m^{-3}$) observed in the open ocean (see Deschamps *et al.*, 1977). The other group corresponds to higher concentrations (up to 3 mg $m^{-3}$) observed in a coastal region of the North Sea (see Viollier *et al.*,

1978b). Combining the two groups, one can find a best-fit regression line for all of the points. Uncertainty in chlorophyll-*a* concentration estimations made with this regression approach is less than one fourth of a log interval, which is acceptable for many biological applications.

The relationships between the difference of reflectances at two wavelengths and the chlorophyll-like pigment content can be approximated with the aid of a theoretical model. It is generally accepted that the diffuse reflectance of the ocean can be written

$$\rho_\lambda = m\frac{b_{0\lambda}}{a_\lambda} + n\frac{b_{p\lambda}}{a_\lambda} \tag{30}$$

where $b_{0\lambda}$ and $b_{p\lambda}$ are the coefficients for scattering due to molecules and particles contained in the water, and $a_\lambda$ is the coefficient for absorption due to pure water and chlorophyll pigments. Viollier *et al.* (1978a) in this way calculated the theoretical variations of $\rho_\lambda$ as a function of particle-scattering coefficient ($b_{p\lambda}$), and as a function of the chlorophyll pigment concentration ($C$), these being the main variables in Equation 30.

By assuming a linear relationship between the particle-scattering coefficient and the chlorophyll concentration, one obtains the theoretical relationship described in Figure 2. The differences between the theoretical and experimental curves are about one fourth of a log interval. We thus have a theoretical model furnishing an approximate relationship between ocean color and chlorophyll-like pigment concentration.

## Atmospheric perturbations

By assuming that the above model is exact, it is proposed that the amplitude of the errors specific to atmospheric effects on chlorophyll retrieval be demonstrated. We have used daily measurements of atmospheric turbidity at an ocean site (Lajes, Azores, see Annex III). A case of low turbidity and a case of high turbidity are considered. The first is characterized by $\tau^A$ (1 μm) = 0.13 and the second by $\tau^A$ (1 μm) = 0.30, values corresponding to the minimum and maximum of the monthly average measurements of $\tau^A$ at this site in 1975. The annual average value $\alpha_m$ for the daily measurements of $\alpha$ was equal to 0.93, and the standard deviation $\Delta\alpha$ around this average was 0.3.

The efficiency of the atmospheric correction algorithm is tested by the following method:

(1) synthetic values of $R$ at 466, 525 and 700 nm are computed for the cases of low and high atmospheric turbidity with $\alpha = 0.93$ and for various chlorophyll-*a* contents between 0.1 and 3 mg $m^{-3}$.

(2) the atmospheric correction algorithm (Equation 26) is applied to the reflectances at 466 and 525 nm, by introducing the values of $\varepsilon$, successively derived from the values of $\alpha = 0.93 \pm \Delta\alpha$. The differences of reflectances $\rho_{466}-\rho_{525}$ are then

TABLE VII

Comparison of initial and retrieval values of the chlorophyll concentration (mg $m^{-3}$) applying the atmospheric correction algorithm. The test is valid for a smooth sea and for turbidity conditions in the Azores Islands (see annex III). Upper part: low turbidity ($\tau^A(1\ \mu m) = 0.13$). Lower part: high turbidity ($\tau^A(1\ \mu m) = 0.3$). The computations were made for $\theta_0 = 41°$ and $\theta = 0°$

| Initial | Retrieval | | Disparsity in log interval unit |
|---|---|---|---|
| | from | to | |
| 0.1 | 0.07 | 0.15 | 0.18 |
| 0.31 | 0.23 | 0.41 | 0.14 |
| 1 | 0.84 | 1.22 | 0.09 |
| 3.13 | 2.75 | 3.66 | 0.06 |
| 0.1 | 0.03 | 0.25 | 0.50 |
| 0.31 | 0.17 | 0.61 | 0.29 |
| 1 | 0.65 | 1.61 | 0.21 |
| 3.13 | 2.24 | 4.49 | 0.15 |

calculated and the chlorophyll content $C$ is deduced. The differences between the initial and retrieved value of $C$ give the uncertainty in $C$ which results from the uncertainty in $\alpha$.

The results of this simulation are found in Table VII. It is noted that the error varies from 0.06 to 0.5 log interval depending upon the atmospheric turbidity and the diversity of the concentrations represented. Accuracy is best for high concentrations, which is explained by the fact that variations of the $\rho_{466} - \rho_{525}$ difference are then mainly due to variations of $\rho_{525}$, which is less subject to the atmospheric effect. It must be remembered that in this case the measurement is primarily of scattering coefficient $b_p$, which is assumed to be correlated with the pigment concentration. For lower concentrations, the correction accuracy is not as good. Just as with the atmospheric uncertainties, there is a 0.2 to 0.5 log interval error, indicating that chlorophyll-like pigment concentration can be estimated to within a factor of 1.5 to 3. Although this uncertainty is large, it nevertheless is consistent with the order of magnitude of other uncertainties encountered in the measurement of chlorophyll pigment concentration. For example, the uncertainty is found to be 0.20 log interval in the case of 'low turbidity', and thus is equal to the uncertainty which commonly is applied to the relationship between optical measurements made at the ocean level and corresponding chlorophyll pigment concentration.

## 7. Conclusion

Atmospheric effects between 400 and 700 nm are of two types: absorption by ozone and scattering by gases and aerosols. A correction for scattering, which is more complicated than a correction ozone absorption, was especially studied in this article.

The following points have been demonstrated:

(1) it is possible to calculate the Rayleigh scattering and the aerosol scattering separately for usual atmospheric turbidity conditions and nearly vertical sightings.

(2) the Rayleigh scattering effects (reflectance and diffuse transmittance) can very accurately be computed as a function of the geometric variables with the aid of simple formulas.

(3) aerosol scattering effects can be linearly extrapolated from one wavelength to another.

The correction algorithm constructed from these results allows the relative ocean reflectance values (ratio of difference of reflectances at two wavelengths) to be retrieved with good accuracy. By supposing that the relationship between the chlorophyll-like pigment concentration and the reflectances in the blue and green at sea level are known, it is shown that the chlorophyll-like pigment concentration can be retrieved to within a factor of 1.5 or 3, depending upon the atmospheric turbidity. These results demonstrate that significant results can be anticipated from visible images of the ocean observed from space.

## ANNEX I

### Absorption by Atmospheric Gases

Absorption between 400 and 700 nm is entirely due to ozone, which is situated high enough in the atmosphere for the absorption and scattering phenomena to be treated separately as follows:

$$R = T_{03}(R_a + \rho T)$$

where $T_{03}$ represents the ozone transmittance and $R_a$, $\rho$ and $T$ are the scattering terms defined in Equation 3.

Transmittance $T_{03}^{\lambda}$ can be given as

$$T_{03}^{\lambda} = \exp\left(-k_{\lambda} U\left(\frac{1}{\mu_0} + \frac{1}{\mu}\right)\right)$$

where $k_{\lambda}$ is the ozone absorption coefficient, and $U$ is the total quantity of ozone in the atmosphere. The only unknown is the quantity of ozone $U$, which is variable in time and space. The average values that are encountered increase from the equator ($U = 0.24$ cm atm) to the poles ($U = 0.38$ cm atm). A seasonal variation is also found, which increases with latitude (see London *et al.*, 1976). In Europe, average values change from 0.28 cm atm in autumn to 0.37 cm atm in spring. The accuracy necessary in the measurement of ozone content is of 0.05 atm cm if an accuracy of 0.002 is to be obtained in the absolute measurement of ocean reflectance. Thus it

seems that the estimation of $T_{03}$ with the aid of the average seasonal ozone content suffices for atmospheric corrections.

## ANNEX II

### Evaluation of the Glitter Reflectance Equivalent

Capillary ripples and waves form a set of variably oriented facets which reflect direct solar radiation in many directions other than the direction of specular reflection. From space this is seen as a glitter pattern which is more or less extensive as a function of surface conditions. Under certain conditions (high sun, rough sea) it is difficult to avoid the reception of some glitter by an ocean color sensor, and this changes the useful signal and is incompatible with application of the atmospheric correction algorithm. It thus is essential that one be able to estimate glitter.

The distribution of surface-reflected solar radiation, and consequentially the wave slope distribution, was studied as a function of wind speed by Cox and Munk (1956). The distribution can be considered approximately isotropic and gaussian, with a variance equal to

$$\sigma^2 = 0.003 + 0.00512\,V \tag{A-1}$$

where $V$ is the wind speed ($\mathrm{m\,s^{-1}}$). The probability function for seeing glitter in direction $(\theta, \phi)$ when the sun is in direction $(\theta_0, \phi_0)$ is thus:

$$p(\theta, \phi; \theta_0, \phi_0, V) = \frac{1}{\pi\sigma^2} \exp\left(-\frac{z_x^2 + z_y^2}{\sigma^2}\right) \tag{A-2}$$

with

$$z_x^2 + z_y^2 = \tan^2 \theta_n \tag{A-3}$$

where $z_x$ and $z_y$ are the components of the slope vector $(\theta_n, \phi_n)$ for which the specular reflection conditions are fulfilled (see Figure 3). With $\omega$ as the reflection angle, $\theta_n$ can be deduced from the following equations

$$\cos 2\omega = \cos\theta \cos\theta_0 + \sin\theta \sin\theta_0 \cos(\phi - \phi_0) \tag{A-4}$$

$$\theta_n = \arccos\left(\frac{\cos\theta + \cos\theta_0}{2\cos\omega}\right). \tag{A-5}$$

Cox and Munk established that the glitter radiance $L_g(\theta, \phi; \theta_0, \phi_0)$ is related to the probability function by the equation

$$L_g(\theta, \phi; \theta_0, \phi_0; V) = \frac{E_0 e^{-\tau/\mu_0}}{4} \frac{1}{\mu\,\mu_0^4} r(\omega) p(\theta, \phi; \theta_0, \phi_0; V) \tag{A-6}$$

where $E_0$ is the solar irradiance at the top of the atmosphere, $\tau$ is the atmospheric optical thickness (Rayleigh, aerosol and ozone), and $r(\omega)$ is the reflection factor given

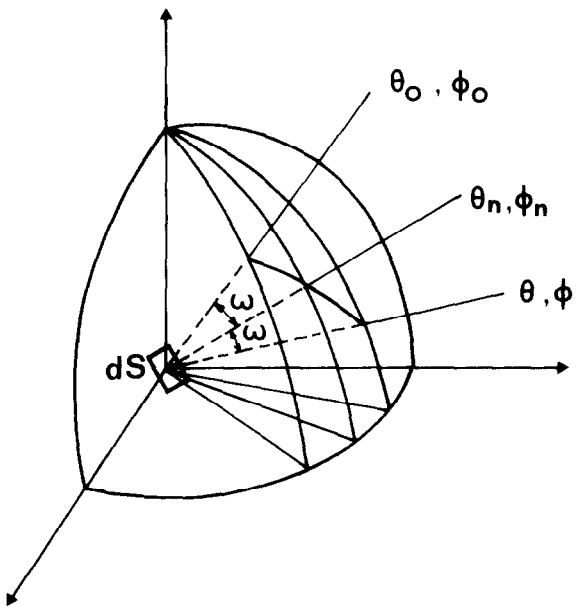


Fig. 3. Reflection geometry.

by Fresnel's law. The glitter reflectance at the top of the atmosphere

$$R_g(\theta, \phi; \theta_0, \phi_0; V) = \frac{\pi L_g(\theta, \phi; \theta_0, \phi_0; V) e^{-\tau/\mu}}{\mu_0 E_0} \tag{A-7}$$

thus can be calculated as a function of $(\theta, \phi)$, $(\theta_0, \phi_0)$ and $V$ by using Equations A–1 through A–6. It must be emphasized that the accuracy of this estimation is dependent upon the validity conditions of the Cox and Munk model. It seems that the model is valid only for homogeneous zones of open sea.

Table A–I shows the $R_g$ values calculated for sighting angles ($\theta = 0, 15, 30, 45°$) in the plane perpendicular to the sun and solar angles ($\theta_0 = 30, 45, 60°$). For these calculations, the atmosphere was considered to be transparent ($\tau = 0$), which leads to a slight overestimation of the results (typically by 30%). It is noted that $R_g$ is negligible ($<10^{-3}$) for solar angles of 45° and 60° when wind speed is low (5 m s$^{-1}$ or 10 kt). Such is no longer the case for a wind speed of 14 m s$^{-1}$ (28 kt). Thus either an exact measurement of glitter radiation, or lacking that, an estimation of wind speed at the sighted zone, seems to be necessary in the ocean color correction algorithms. When the wind speed is known to be low (typically less than 5 m s$^{-1}$), glitter reflectance can be ignored and the atmospheric correction algorithm described in this paper can be applied without modification.

TABLE A-I

Reflectance of glitter in a plane perpendicular to the plane of incidence. Windspeeds are 5 and 14 m $s^{-1}$.

| $v = 5$ m/s $\theta$ \ $\theta_0$ | 30 | 45 | 60 |
|---|---|---|---|
| 0 | 0.0189 | 0.0009 | 0.0000 |
| 15 | 0.0093 | 0.0003 | 0.0000 |
| 30 | 0.0009 | 0.0000 | 0.0000 |
| 45 | 0.0000 | 0.0000 | 0.0000 |

| $v = 14$ m/s $\theta$ \ $\theta_0$ | 30 | 45 | 60 |
|---|---|---|---|
| 0 | 0.0341 | 0.0133 | 0.0029 |
| 15 | 0.0273 | 0.0096 | 0.0017 |
| 30 | 0.0132 | 0.0033 | 0.0003 |
| 45 | 0.0033 | 0.0004 | 0.0000 |

# ANNEX III

## Statistical Study of Atmospheric Turbidity

Aerosol optical thickness depends on wavelength according to a power law characterized by coefficient $\alpha$

$$\tau^A(\lambda_1) = \tau^A(\lambda_0)\left(\frac{\lambda_1}{\lambda_0}\right)^{-\alpha}.$$

The parameters characterizing atmospheric turbidity thus are $\alpha$ and $\tau^A(\lambda_0)$ where $\lambda_0$ is a reference wavelength, generally 1 μm.

The measurement of the optical thickness $\tau^A(\lambda)$ is deduced from the measurement of direct solar radiation $E_{s\lambda}$ by using the Lambert–Bouguer law

$$E_{s\lambda} = E_{0\lambda} \exp\left(-(\tau^M + \tau^G + \tau^A)m\right)$$

where $E_{0\lambda}$ is solar irradiance at the top of the atmosphere; $\tau^M$ = Rayleigh optical thickness; $\tau^G$ = absorption optical thickness (ozone); and $m$ = air mass.

Coefficient $\alpha$ is deduced from measurements at two wavelengths

$$\alpha = \frac{\ln\left(\tau^A(\lambda_1)/\tau^A(\lambda_0)\right)}{\ln\left(\lambda_0/\lambda_1\right)}.$$

These measurements are made daily at some of the World Meteorological Organization network stations and are published (Anonymous 1977). From these data, those for the Lajes site (38°45 N, 27°05 W) were selected, as they are representative of oceanic conditions. Table A-II shows the monthly averages for $\tau^A$

TABLE A-2

Monthly averages for atmospheric turbidity parameters $\tau^A(1\ \mu m)$ and $\alpha$. Measurements made in Lajes, Azores (38° 45N, 27° 05W) obtained from Anonymous (1977)

| Month | Number of measurements | $\tau^A(1\ \mu m)$ | $\alpha$ |
|---|---|---|---|
| J | 9 | 0.126 | 1.080 |
| F | 5 | 0.154 | 1.093 |
| M | 5 | 0.195 | 1.074 |
| A | 5 | 0.308 | 0.781 |
| M | 37 | 0.241 | 1.031 |
| J | 20 | 0.203 | 1.145 |
| J | 24 | 0.299 | 0.894 |
| A | 30 | 0.242 | 1.014 |
| S | 23 | 0.253 | 0.877 |
| O | 14 | 0.233 | 0.829 |
| N | 6 | 0.199 | 0.609 |
| D | 4 | 0.212 | 0.771 |

(1 μm) and $\alpha$. The turbidity minimum is observed in January ($\tau^A(1\ \mu m) = 0.13$), whereas two maxima are observed, in April and July ($\tau^A(1\ \mu m) = 0.3$). The annual average and variance of $\alpha$ respectively are equal to 0.93 and 0.3. The range of $\alpha$ variation thus is relatively small for ocean sites.

## Acknowledgments

This research was supported by the 'Centre National de la Recherche Scientifique' (C.N.R.S.) and by the 'Centre National d'Etudes Spatiales' (C.N.E.S.).

The authors wish to thank Dr. M. Herman and J. Lenoble for introducing them to the subject and for their helpful assistance, and L. F. Martin for his aid in the translation of this paper.

## References

Anonymous: 1977, 'Global Monitoring of the Environment for Selected Atmospheric Constituents 1975', *Environmental Data Service – Asheville* NC 28801 U.S.A.

Arvesen, J. C., Millard, J. P., and Weaver, E. C.: 1973, 'Remote Sensing of Chlorophyll and Temperature in Marine and Fresh Waters', *Astronaut. Acta* **18**, 229–239.

Box, M. A., and Lo, S. Y.: 1976, 'Approximate Determination of Aerosol Size Distribution', *J. Appl. Meteorol.* **15**, 1068–1076.

Clarke, G. L., Ewing, G. C., and Lorensen, C. J.: 1970, 'Spectra of Backscattered Light from the Sea Obtained from Aircraft as a Measure of Chlorophyll Concentration', *Science* **167**, 1119–1121.

Cox, C., and Munk, W.: 1965, 'Slopes of the Sea Surface Deduced from Photographs of Sun Glitter', *Bull. Scripps Inst. Oceanogr. Univ. Calif.* **6**, 401–488.

Curran, R. I.: 1972, 'Ocean Color Determination through a Scattering Atmosphere', *Appl. Opt.* **11**, 1857–1866.

Deschamps, P. Y., Lecomte, P., and Viollier, M.: 1977, 'Remote Sensing of Ocean Color and Detection of Chlorophyll Content', *Proc. 11th Int. Symp. on Remote Sensing of Environment, Ann Arbor*, 1021–1033.

Gordon, H. R.: 1978, 'Removal of Atmospheric Effects from Satellite Imagery of the Oceans', *Appl. Opt.* **17**, 1631–1636.

Hovis, W. A., Forman, M. L., and Blaine, L. R.: 1973, 'Detection of Ocean Color Changes from High Altitude', *NASA* X–652–73–371.

Hovis, W. A.: 1978, 'The Coastal Zone Color Scanner (CZCS) Experiment', *The Nimbus 7 Users' Guide NASA*, G.S.F.C.

Hoyt, D. V.: 1977, 'A Redetermination of the Rayleigh Optical Depth and its Application to Selected Solar Radiation Problems', *J. Appl. Meteorol.*, **16**, 432–436.

Kattawar, G. W., and Humphreys, T. I.: 1976, 'Remote Sensing of Chlorophyll in an Atmosphere–Ocean Environment: A Theoretical Study', *Appl. Opt.* **15**, 273–282.

London, J., Bojkov, R. D., Oltsùans, S., and Kelly, J. I.: 1976, 'Atlas of the Global Distribution of Total Ozone', *NCAR/TN/133 + STR.*

McClatchey, R. A., Fenn, R. W., Selby, J. E. A., Voltz, F. E., and Garine, J. S.: 1971, 'Optical Properties of the Atmosphere', *AFCRL 71–0279 Envir. Res. Papers No. 354.*

Miller, J. R., Jain, S. C., O'Neill, N. T., McNeil, W. R., and Thompson, K. P. B.: 1977, 'Interpretation of Airborne Spectral Reflectance Measurements over Georgian Bay', *Remote Sensing Environ.* **6**, 183–200.

Plass, G. N., Kattawar, G. W., and Hitzfelder, S. J.: 1976, 'Multiple Scattered Radiation Emerging from Rayleigh and Continental Haze Layers. 1: Radiance, Polarization and Neutral Points', *Appl. Optics*, **15**, 632–647.

Sekera, Z., and Kahle, A. B.: 1966, 'Scattering Functions for Rayleigh Atmospheres of Arbitrary Thickness', *Rand Report R–452–PR.*

Tanré, D., and Herman, M.: 1978, 'Correction de l'effet de diffusion atmosphérique pour les données de télédétection', *Proceedings of an Int. Conf. on Earth Observation held at Toulouse ESA–SP 134*, 355–360.

Viollier, M., Deschamps, P. Y., and Lecomte, P.: 1978a, 'Airborne Remote Sensing of Chlorophyll Content under Cloudy Sky as Applied to the Tropical Waters in the Gulf of Guinea', *Remote Sensing of Environ.* **7**, 235–248.

Viollier, M., Lecomte, P., Bougard, M., and Richard, A.: 1978b, 'Expérience aéroportée de télédétection (température et couleur de la mer) dans le détroit du Pas de Calais, *Oceanologica Acta*, **1**, 265–269.

Wilson, W. M., Austin, R. W., and Smith, R. C.: 1978, 'Optical Remote Sensing of Chlorophyll in Ocean Waters', *Proc. of the 12th Int. Symp. on Remote Sensing of Environment* (Manila), 1103–1113.